Molecular Therapy
Methods & Clinical Development
Original Article

Induction of ER Stress by an AAV5 BDD FVIII Construct Is Dependent on the Strength of the Hepatic-Specific Promoter

Sylvia Fong,[1] Britta Handyside,[1] Choong-Ryoul Sihn,[1] Su Liu,[1] Lening Zhang,[1] Lin Xie,[1] Ryan Murphy,[1] Nicole Galicia,[1] Bridget Yates,[1] Wesley C. Minto,[1] Catherine Vitelli,[1] Danielle Harmon,[1] Yuanbin Ru,[1] Guoying Karen Yu,[1] Claudia Escher,[2] Jakob Vowinckel,[2] Jill Woloszynek,[1] Hassib Akeefe,[1] Rajeev Mahimkar,[1] Sherry Bullens,[1] and Stuart Bunting[1]

[1]BioMarin Pharmaceutical, Inc., Novato, CA, USA; [2]Biognosys AG, Schlieren, Switzerland

Adeno-associated virus 5 (AAV5)-human factor VIII-SQ (hFVIII-SQ; valoctocogene roxaparvovec) is an AAV-mediated product under evaluation for treatment of severe hemophilia A, which contains a B-domain-deleted hFVIII (hFVIII-SQ) transgene and a hybrid liver-specific promotor (HLP). To increase FVIII-SQ expression and reduce the vector dose required, a stronger promoter may be considered. However, because FVIII-SQ is a protein known to be difficult to fold and secrete, this could potentially induce endoplasmic reticulum (ER) stress. We evaluated the effect of two AAV5-hFVIII-SQ vectors with different liver-specific promoter strength (HLP << 100ATGB) on hepatic ER stress in mice. Five weeks after receiving vehicle or vector, the percentage of transduced hepatocytes and levels of liver hFVIII-SQ DNA and RNA increased dose dependently for both vectors. At lower doses, plasma hFVIII-SQ protein levels were higher for 100ATGB. This difference was attenuated at the highest dose. For 100ATGB, liver hFVIII-SQ protein accumulated dose dependently, with increased expression of ER stress markers at the highest dose, suggesting hepatocytes reached or exceeded their capacity to fold/secrete hFVIII-SQ. These data suggest that weaker promoters may require relatively higher doses to distribute expression load across a greater number of hepatocytes, whereas relatively stronger promoters may produce comparable levels of FVIII in fewer hepatocytes, with potential for ER stress.

INTRODUCTION

Hemophilia A is an X-linked hereditary hemorrhagic disorder characterized by deficiency or dysfunction of coagulation protein factor VIII (FVIII). It has a prevalence of 1 in 5,000 male live births, and affected individuals can present with mild, moderate, or severe phenotype.[1] In the severe form, recurrent joint and muscle bleeds lead to progressive and debilitating musculoskeletal damage. The current standard of care for severely affected individuals is "episodic" or frequent (2 or 3 times per week), potentially burdensome prophylactic administration of recombinant or plasma-derived clotting FVIII. This approach can be further complicated by the development of neutralizing antibodies.[2,3] Whereas injected FVIII replacement may remain an important therapeutic option, recent advances in gene therapy could revolutionize disease management in hemophilia A.[4–9]

Adeno-associated virus 5 (AAV5)-human FVIII-SQ (hFVIII-SQ; valoctocogene roxaparvovec) is a gene therapy being developed for the treatment of severe hemophilia A, comprising a replication-incompetent AAV5 vector containing a B-domain-deleted (BDD) human FVIII gene (hFVIII-SQ) driven by a hybrid liver-specific promoter (HLP).[10] To be an effective therapeutic, it is crucial that the vector reaches the liver, is taken up by hepatocytes, the DNA is processed and expressed, and the FVIII protein is correctly folded prior to secretion. However, BDD FVIII transgenes produce FVIII-SQ protein that is inefficiently folded and secreted from the endoplasmic reticulum (ER).[11,12] The B-domain facilitates FVIII transit through the ER to the Golgi via interactions with ER chaperones.[13] For this reason, codon-optimized FVIII variants, such as recombinant AAV (rAAV)-HLP-codop-hFVIII-V3, have been developed to increase FVIII secretion.[14] There has also been a concern that an adaptive acute unfolded protein response (UPR) may be activated in instances of increased expression, leading to ER stress.[15,16] Early data suggested that *in vivo* hydrodynamic delivery of plasmids that encode full-length or BDD-FVIII proteins may induce an UPR in murine hepatocytes, resulting in apoptosis.[11] More recent studies in mice showed evidence of a cellular stress response in animals treated with a BDD-FVIII transgene via an AAV serotype 8 vector; however, this was not augmented at high vector doses nor was there any indication of hepatotoxicity or heightened immune response to FVIII, even at supraphysiological levels of FVIII expression.[15] Similarly, in a mouse model of hemophilia A treated with valoctocogene roxaparvovec

Received 6 April 2020; accepted 6 July 2020;
https://doi.org/10.1016/j.omtm.2020.07.005.

Correspondence: Sylvia Fong, BioMarin Pharmaceutical, Inc., 105 Digital Drive, San Rafael, CA 94949, USA.
E-mail: sfong@bmrn.com

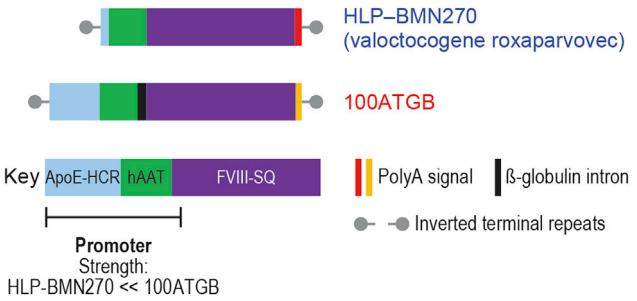

Figure 1. Human FVIII Constructs

Component diagram of the HLP-BMN270 and 100ATGB constructs. Each vector contained a HLP of differing strength—either HLP-BMN270 or the stronger promoter, 100ATGB. ApoE-HCR, apolipoprotein E-hepatic control region; hAAT, human alpha-1-antitrypsin; hFVIII-SQ, human B-domain-deleted clotting factor VIII; HLP, hybrid liver-specific promoter; PolyA, polyadenylation (synthetic polyamide signal for HLP-BMN270 and bovine growth hormone polyadenylation signal for 100ATGB vector).

(AAV5-based BDD-FVIII transgene), normal to supraphysiological levels of plasma hFVIII-SQ were achieved, with fully corrected bleeding time and no evidence of liver dysfunction or hepatocyte ER stress.[10] Similarly, in human subjects with severe hemophilia A in a phase-I/II dose-ranging study of valoctocogene roxaparvovec, there was no clear evidence of liver dsyfunction.[9] In addition, this clinical study showed that a single infusion of valoctocogene roxaparvovec at 6×10^{13} vg/kg provided sustained normalization of FVIII activity level over 1 year and profound reduction in injected FVIII use.[9]

Nevertheless, in instances where increased FVIII-SQ protein expression might be desired at lower vector doses, a stronger promoter may be considered. This approach could potentially produce larger amounts of hFVIII-SQ protein per cell, increasing potential for induction of ER stress and UPR, possibly compromising the duration of efficacy and patient safety. Therefore, we performed this preclinical study in mice to compare the effect of 2 AAV5 hFVIII-SQ vector constructs with liver-specific promoters of markedly different strength (i.e., HLP versus 100ATGB, the latter a stronger promoter). We evaluated hepatocellular production of hFVIII-SQ and examined the capacity of the liver to fold and secrete the hFVIII-SQ protein, using the sentinel molecular chaperone 78 kDa glucose-regulated protein (GRP78)/binding immunoglobulin protein as a biomarker.

RESULTS

Promoter Strength and Plasma and Liver hFVIII Expression

8-week-old male *RAG2*$^{-/-}$ mice received a single intravenous bolus injection of either of 2 AAV5-based vectors at 6×10^{12}, 2×10^{13}, or 6×10^{13} vg/kg. Each vector contained a liver-specific promoter of differing strength: HLP (AAV5-HLP-hFVIII-SQ; valoctocogene roxaparvovec) or the stronger promoter 100ATGB (AAV5-100ATGB-hFVIII-SQ) (Figure 1).

Expression of hFVIII-SQ DNA, RNA, and protein levels was systematically assessed for each construct. Analyses of hFVIII-SQ DNA performed using quantitative polymerase chain reaction (qPCR) and *in situ* hybridization (ISH) showed that dose-dependent increases in liver hFVIII-SQ DNA were evident for both promoters (Figure 2A). With the use of ISH analysis, hFVIII-SQ DNA was shown to be present, to a greater extent, in hepatocytes of the peri-central regions of the liver lobules than in peri-portal regions for both constructs at lower doses (Figure 2B). At the 6×10^{13} vg/kg dose, almost all of the hepatocytes stained positive for hFVIII-SQ vector DNA (Figure 2C). There was no difference in the amount of FVIII-SQ DNA measured by qPCR or the percentage of hepatocytes transduced between the 2 constructs at equivalent doses. In addition, there were also dose-dependent increases in liver hFVIII-SQ RNA (Figure 2D) for both promoters. At all doses tested, more hFVIII-SQ RNA transcript per unit DNA was detected in the 100ATGB groups, confirming 100ATGB as the stronger promoter (Figure 2E).

Interestingly, at the 2 lower doses of vectors studied, plasma levels of hFVIII-SQ protein were consistently higher for the 100ATGB construct than for the HLP construct. However, at 6×10^{13} vg/kg, circulating levels of hFVIII-SQ protein were attenuated in the 100ATGB group and were comparable with the HLP cohort (Figure 2F). To understand the mechanism responsible for attenuation of plasma hFVIII-SQ protein levels at high-dose 100ATGB, liver FVIII-SQ protein levels were analyzed by immunohistochemistry (IHC) and enzyme-linked immunosorbent assay (ELISA). Similar to FVIII-SQ DNA, there was a dose-dependent increase in the proportion of hepatocytes that stained positive for FVIII-SQ protein (Figures 2G and 2H). However, there was a marked accumulation of hFVIII-SQ protein in the liver of mice treated with 6×10^{13} vg/kg of the stronger 100ATGB construct compared with the HLP construct (Figure 2I). This difference was particularly evident in the central vein region of the hepatic lobules (Figure 2H), which is consistent with previous studies.[10] The markedly higher hepatic RNA/DNA ratio for 100ATGB corresponded to a dose-dependent decrease in the amount of secreted FVIII protein per unit RNA (Figure 2J).

Unfolded Protein Response (UPR)

As different degrees of hFVIII-SQ protein retention were observed in the peri-central regions of the liver following treatment with HLP and 100ATGB constructs at 6×10^{13} vg/kg, markers of the UPR were evaluated in liver homogenates and formalin-fixed sections. Levels of GRP78, spliced X-box binding protein 1 (XBP1s), CCAAT/enhancer-binding protein homologous protein (CHOP), and activated caspase-3 were measured in liver homogenates by reverse transcription droplet digital PCR (RT-ddPCR), IHC, or ELISA. Administration of the HLP or 100ATGB constructs at 6×10^{13} vg/kg did not result in changes in XBP1s or CHOP expression versus vehicle controls. Moreover, there was no change in the level of active caspase-3 protein over vehicle control (Figures 3A–3C). The positive controls, tunicamycin, thapsigargin, or staurosporine (known inducers of ER stress), each induced a marked increase in XBP1s and CHOP expression and active caspase-3 protein. Plasma alanine aminotransferase (ALT) levels were normal in all treatment groups (Figure S1).

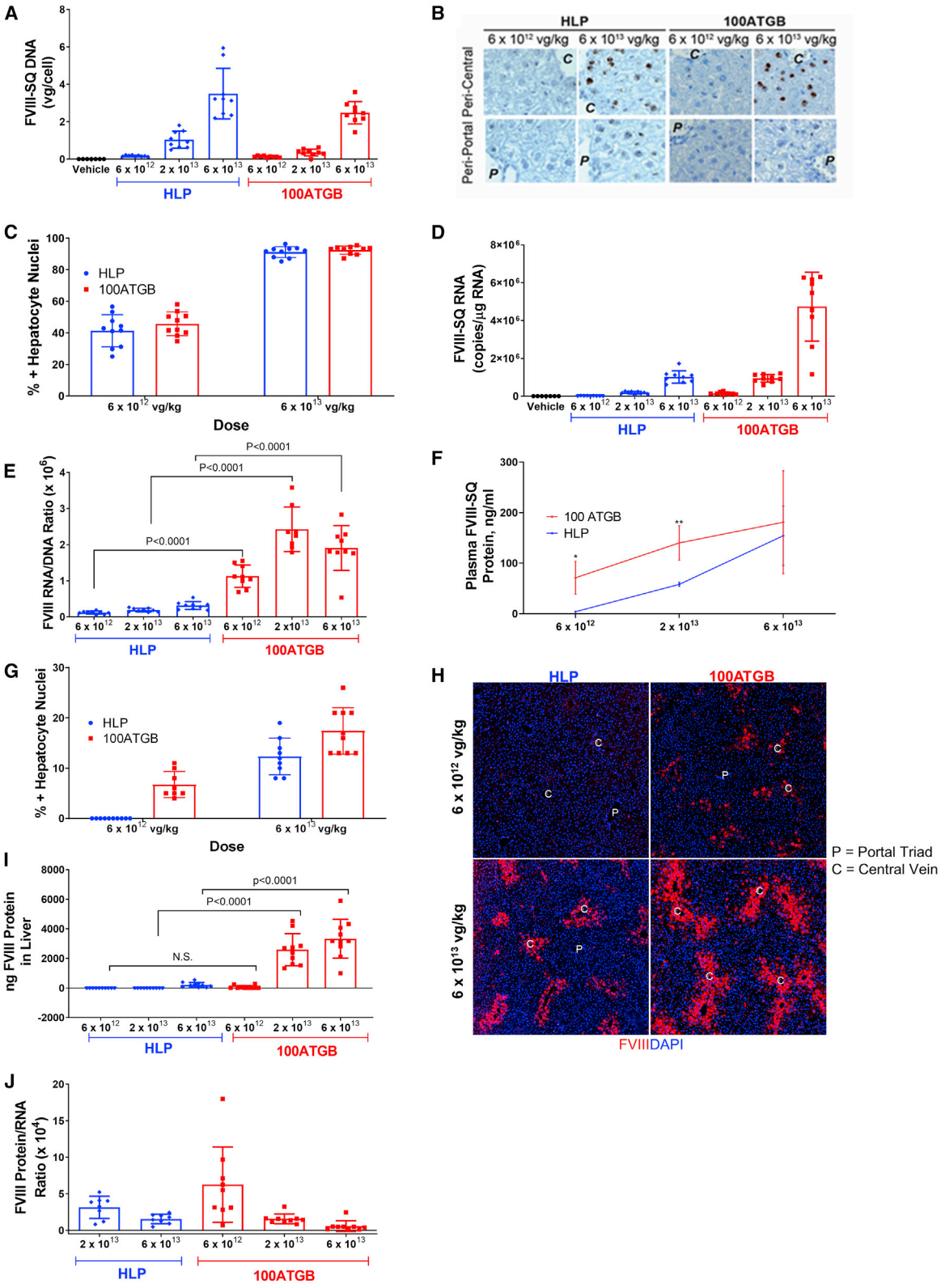

(legend on next page)

Notably, administration of the 100ATGB construct at the 6×10^{13} vg/kg dose was associated with significantly increased hepatic expression and percentage of hepatocytes staining positive for GRP78 versus vehicle control ($p < 0.005$) (Figures 3D and 3E). By contrast, there was no significant increase in hepatic expression and the percentage of hepatocytes staining positive for GRP78 at the comparable dose of 6×10^{13} vg/kg HLP, suggesting induction of UPR occurs only with the stronger promoter. This was shown by more intense immunofluorescence staining of GRP78 proteins in hepatocytes that stained positive for the FVIII protein (Figure 3F).

Hyper-Reaction Monitoring (HRM) Proteomic Analysis

As increased levels of hepatic GRP78 were observed in 100ATGB-treated mice at the high-dose level, HRM-based mass spectrometry proteomic analysis was performed in liver samples from animals treated with the 100ATGB construct at 6×10^{12} or 6×10^{13} vg/kg. Animals that received the higher 100ATGB dose showed significantly increased expression of key activating transcription factor 6 (ATF6)-mediated molecular chaperone proteins versus controls (Figures 4A–4D); these included protein disulfide isomerase family A member 4 (PDIA4; $p < 0.0001$), mesencephalic astrocyte-derived neurotrophic factor (MANF; $p < 0.005$), DNAJ homolog subfamily C member 3 (DNAJC3; $p < 0.005$), and GRP78 (also known as heat shock protein family A [HSP70] member 5 [HSPA5], $p < 0.005$) (Figures 4A–4D). Other upregulated chaperone proteins included hypoxia-upregulated 1 protein (HYOU1), PDIA3, and cysteine-rich with epidermal growth factor-like domains 2 (Figure S2). Collectively, these observations suggest that the upregulation of key ATF6-mediated molecular chaperone proteins might be occurring primarily via the adaptive molecular chaperone pathway (Figure 4E).

Given the role of GRP78 as a molecular chaperone, we hypothesized that higher levels of liver GRP78 would aid hepatocytes in the folding and secretion of more FVIII-SQ protein and that the increased GRP78 expression observed in the 6×10^{13} vg/kg dose of the 100ATGB group was an adaptive response to the increased FVIII-SQ protein expression seen with this promoter. Supporting this hypothesis, following administration of the 100ATGB construct, significant positive associations were observed between circulating plasma hFVIII-SQ protein levels and the hepatic expression of GRP78, along with other molecular chaperones, including PDIA5, PDIA6, HYOU1, and stromal cell-derived factor 2-like protein 1 (SDF2L1); all p and R values < 0.05 and ≥ 0.66, respectively. No association was seen for housekeeping protein ribosomal protein lateral stalk subunit P0 (RPLP0) (Figures 5A–5F). Next, we asked whether the plasma GRP78 level could be used as a biomarker to correlate hepatic capacity to fold and secrete FVIII-SQ proteins. In these studies, consistent with liver GRP78 protein, plasma levels of GRP78 were significantly increased in mice treated with the 100ATGB construct at the 6×10^{13} vg/kg dose ($p = 0.0067$) (Figure 6A). Moreover, plasma levels of GRP78 protein were positively correlated with levels of GRP78 in the liver ($p < 0.01$, $R = 0.563$) and with circulating plasma levels of hFVIII-SQ ($p < 0.01$, $R = 0.648$) (Figures 6B and 6C). Correlation between plasma levels of GRP78 and hFVIII-SQ remained significant if the 6×10^{13} vg/kg dose of 100ATGB alone was analyzed ($p < 0.05$, $R = 0.639$).

DISCUSSION

To date, there is no evidence of liver dysfunction or ER stress in mice treated with valoctocogene roxaparvovec at doses that produce normal to supraphysiological levels of hFVIII-SQ. A strong promoter, such as 100ATGB, may allow increased hFVIII-SQ expression in the clinic using lower vector doses. The findings reported here demonstrate that use of the 100ATGB promoter in the AAV5-derived BDD hFVIII-SQ vector construct provided higher levels of both hepatic and circulating hFVIII-SQ protein in mice compared with the HLP construct, confirming that 100ATGB is the stronger promoter. However, hepatic accumulation of hFVIII-SQ protein and apparent leveling off of circulating hFVIII-SQ at a higher 100ATGB vector dose, together with an associated dose-dependent decrease in plasma hFVIII-SQ protein per unit hFVIII-SQ RNA, suggested that with the stronger promoter, hepatocytes may approach or exceed their capacity to fold and secrete the hFVIII-SQ protein effectively. Endogenous FVIII is primarily synthesized by liver sinusoidal endothelial cells rather than hepatocytes.[17,18] This may play a role in the limited capacity of hepatocytes to fold and secrete FVIII effectively, and overexpression of hFVIII-SQ by hepatocytes may result in ER stress.[11] Induction of an adaptive UPR is a protective mechanism, shielding cells against injury.[19] However, overactivation or chronic prolongation of UPR may lead to apoptosis and loss of hepatocytes.[10] Several pathways can contribute to ER stress-mediated apoptosis, including inositol-requiring enzyme 1α (IRE1α), apoptosis signal-regulating kinase 1, c-Jun N-terminal kinases signaling, CHOP regulation of B cell lymphoma 2 (BCL2) protein family members and apoptotic genes, ER-localized BCL2-associated X protein, BCL2 homologous antagonist killer, and glycogen synthase kinase 3β (GSK3β).[20] Under such conditions, protein load on the ER may greatly exceed its folding capacity, resulting in cellular dysfunction and cell death.[20]

Figure 2. Effect of Promoter on FVIII Expression

Effect of promoter on FVIII-SQ DNA, RNA, and protein expression. (A–C) The effect of promoter on hFVIII-SQ DNA in the liver was measured by (A) qPCR and (B and C) *in situ* hybridization (IHC). (B) Representative IHC image. (C) Percentage of FVIII positive hepatocyte nuclei counted from IHC images. (D) The effect of promoter on hFVIII-SQ RNA was measured by qPCR. (E) Ratio of RNA transcript per unit DNA was compared between promoters and doses. (F) Circulating levels of hFVIII-SQ proteins in the plasma were analyzed by ELISA. (G–I) Protein staining in the liver was analyzed using (G and H) IHC and (I) ELISA. (J) Ratio of FVIII protein expression in plasma per unit liver RNA was compared between promoters and doses. Studies in *RAG2*$^{-/-}$ mice, 5 weeks following a single tail-vein administration of vehicle, AAV5-HLP-hFVIII-SQ (HLP), or AAV5-100ATGB-hFVIII-SQ (100ATGB) construct at 6×10^{12}, 2×10^{13}, or 6×10^{13} vg/kg. Nuclei were counted positive for any signal, i.e., irrespective of DNA amount. Results are mean ± SD, n = 7–10 per group. *$p < 0.05$, **$p < 0.005$ 100ATG versus HLP. 100ATGB, AAV5-100ATGB-hFVIII-SQ; DAPI, 4′,6-diamidino-2-phenylindole; ELISA, enzyme-linked immunosorbent assay; FVIII, factor VIII; HLP, hybrid liver-specific promoter; IHC, immunohistochemistry; qPCR, quantitative PCR; SD, standard deviation.

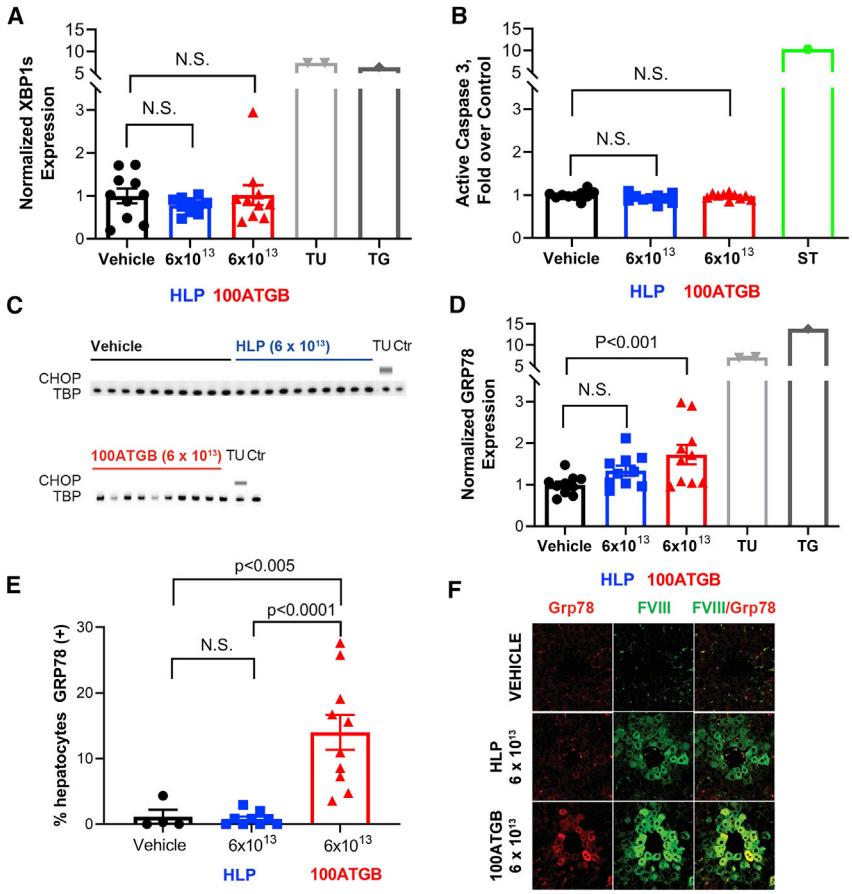

Figure 3. Unfolded Protein Response by Construct

Markers of UPR were evaluated in liver homogenate and formalin-fixed sections. (A) Normalized XBP1 expression was measured among promoters, positive controls, and vehicle control by RT-ddPCR. (B) Active caspase-3 XBP1 expression was measured among promoters, positive controls, and vehicle control by ELISA. (C) CHOP expression was analyzed by western blot. (D–F) GRP78 expression was analyzed by (D) RT-ddPCR and (E and F) IHC. Results are mean ± SEM, n = 4–10 per group. CHOP, C/EBP homologous protein; Ctr, control; ELISA, enzyme-linked immunosorbent assay; HLP, hybrid liver-specific promotor; IHC, immunohistochemistry; N.S., not significant; RT-ddPCR, reverse transcription droplet digital PCR; SEM, standard error of mean; TBP, TATA-box binding protein; Tu, tunicamycin; UPR, unfolded protein response; XBP1s, spliced X-box binding protein 1.

In this study, following administration of the 100ATGB construct, significant positive associations were observed between circulating plasma hFVIII-SQ protein levels and the hepatic expression of GRP78, PDIA5, PDIA6, HYOU1, and SDF2L1, suggesting that the hepatic capacity to fold and secrete proteins could affect the levels of circulating FVIII. Moreover, the observed associations between plasma hFVIII-SQ levels and increased hepatic expression of molecular chaperones suggest that the stronger 100ATGB construct at the highest 6×10^{13} vg/kg dose induces an adaptive UPR. One component of this adaptive mechanism, GRP78, is a master regulator of ER homeostasis and stress responses, with its synthesis markedly induced under conditions that lead to the accumulation of unfolded polypeptides in the ER.[21] GRP78 may directly interact with FVIII-SQ, and ATP-dependent disassociation from GRP78 may be important for FVIII secretion.[22] Thus, the observed increased expression of the sentinel chaperone protein GRP78, along with various other downstream ATF6-mediated molecular chaperones, lends support for an adaptive UPR, although the increase was relatively modest compared with the chemically induced positive controls and consistent with previous reports.[10] Notably, the lack of any increase in other ER stress markers, including XBP1s, active caspase-3, and CHOP, in liver homogenates or in plasma ALT level suggests that the response to the high dose of the 100ATGB construct did not result in measurable hepatocyte damage or apoptosis. In addition, the observed associations between plasma GRP78 and plasma FVIII levels suggest that the level of plasma GRP78 and possibly other ATF6-mediated chaperones may reflect the ability/capacity of the liver to fold the FVIII protein, a crucial step in the attainment of appropriate plasma FVIII levels. Increased circulating GRP78 levels are associated with hepatocellular carcinoma and liver damage caused by cholestasis, as well as nonhepatic conditions, such as obesity, metabolic disorders, rheumatoid arthritis, and lung cancer.[23–29] Under normal conditions, GRP78 is associated with IRE1 and protein kinase RNA-like ER kinase (PERK).[30,31] However, GRP78 dissociates from IRE1α and PERK, resulting in the activation of IRE1α and PERK that lead to proapoptotic pathways/mechanisms in conditions of prolonged and unresolved ER stress.[31,32] Unlike in high ER stress conditions, the moderate increase in GRP78 in this study suggests a protective, rather than apoptotic, effect. FVIII forms protein aggregates in the ER that can disaggregate, refold, and be secreted as functional FVIII.[33] GRP78 also significantly reduces both wild-type-FVIII and BDD-FVIII protein aggregation, which allows FVIII to be properly folded and secreted.[33]

Although *in vitro* and *in vivo* overexpression of FVIII can result in activation of the UPR and apoptosis, this may be dependent on promotor strength, codon optimization, and choice of FVIII construct.[10,11] Administration of 6×10^{13} vg/kg AAV5-hFVIII-SQ vector in mice caused minimal retention of hFVIII-SQ in hepatocytes, without significant changes in levels of GRP78, XBP1, ATF6, and CHOP detected in liver homogenates, collected 5, 12, and 24 weeks postdosing.[10] Higher doses (up 2×10^{14} vg/kg) did not change liver expression of active caspase-3, plasma aspartate aminotransferase, or plasma ALT in mice, 8 weeks postdosing.[10] Mild, nonserious, and transient elevations in ALT levels were reported in 15 adults with severe hemophilia who had received a single infusion of AAV5-hFVIII-

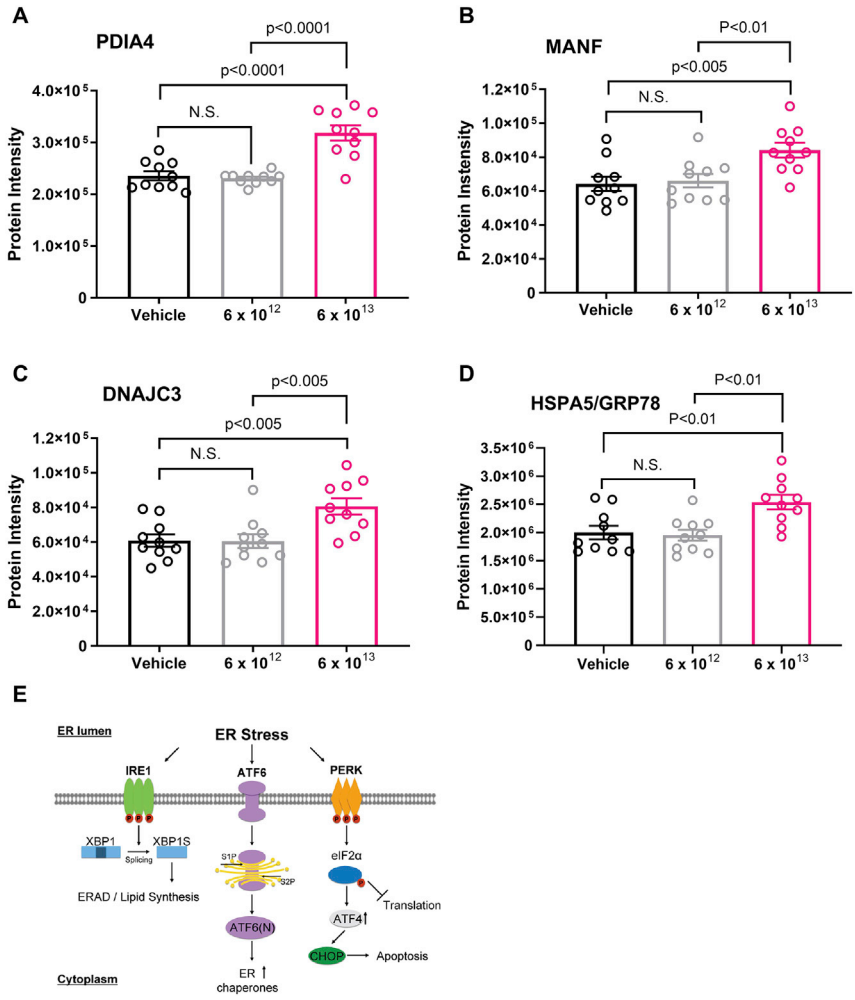

Figure 4. 100ATGB Induction of ATF6-Mediated Molecular Chaperone Expression

HRM-based mass spectrometry proteomic analysis was performed in liver samples from animals treated with the 100ATGB construct at 6×10^{12} or 6×10^{13} vg/kg. (A–D) Expression of key ATF6-mediated molecular chaperone proteins was analyzed versus controls, including (A) PDIA4, (B) MANF, (C) DNAJC3, and (D) GRP78. (E) Diagram of the adaptive molecular chaperone pathway. Statistics calculated via ANOVA, followed by multiple comparison adjustment. Results are mean ± SEM, n = 10 per group. ATF4, activating transcription factor 4; ATF6, activating transcription factor 6; CHOP, CCAAT/enhancer-binding protein homologous protein; DNAJC3, DNAJ homolog subfamily C member 3; EIF2α, eukaryotic translation initiation factor 2-alpha; ER, endoplasmic reticulum; ERAD, endoplasmic reticulum-associated lipid degradation; GRP78, 78 kDa glucose-regulated protein; HRM, hyper-reaction monitoring; HSPA5, heat shock protein family A (HSP70) member 5; IRE1α, inositol-requiring enzyme 1α; MANF, mesencephalic astrocyte-derived neurotrophic factor; N.S., not significant; PDIA4, protein disulfide isomerase family A member 4; SEM, standard error of mean; XBP1, X-box binding protein 1; XBP1s, spliced X-box binding protein 1.

SQ at various dose levels.[34] However, the levels were not indicative of ongoing liver damage, and the authors did not note evidence of ER stress and were unable to attribute the levels to abnormal hepatocyte turnover.[34] Pre- and post-treatment human liver biopsies are necessary to confirm the presence or absence of UPR activation in humans after FVIII gene therapy.

To our knowledge, this is the first study to demonstrate directly the secretion of GRP78 associated with GRP78 expression in liver. For HLP, levels of hepatic and circulating FVIII protein were lower than for 100ATGB, and there was no evidence of an UPR at any HLP vector dose tested, even at the highest dose used in a clinical setting. These findings are consistent with normal plasma ALT levels and the earlier reported lack of increase in active capase-3 in liver homogenate in mice that were administered a very high-dose (2×10^{14} vg/kg) valoctocogene roxaparvovec.[10] Future studies should assess whether overexpression of FVIII affects its glycosylation, since abnormal glycosylation in missense mutant forms of FVIII was shown to alter FVIII protein folding, trafficking, and secretion.[35,36]

It is unclear if the use of a lower vector dose with a stronger promoter would provide meaningful FVIII levels for the treatment of hemophilia A in humans. The levels achieved in the mouse with the stronger promoter at 2E13 are ~100 ng/mL, which is ~65% of normal FVIII activity. However, expression level may be lower in humans. Specifically, plasma FVIII levels were approximately 3.7-fold lower in humans when comparing mouse steady-state and human peak concentrations following AAV5-FVIII-SQ administration.[10] Therefore, the level observed in mice with the stronger promoter in this study would likely translate to a 2- to 3-fold lower peak activity in humans. However, the combination of a lower dose and stronger promoter might be possible with an easier-to-secrete form of FVIII (e.g., hFVIII-V3).[14]

Limitations of gene therapy include transient elevation of liver transaminases resulting from an immune response to the vector capsid, underlying liver disease, and development of neutralizing antibodies to clotting factors.[3,6,37] Prednisolone treatment is frequently administered to minimize potential immune-mediated hepatocyte injury.[9] In this study, no significant increases in plasma ALT were apparent for either vector at any dose, implying no hepatocyte injury under the conditions tested.

Conclusion

Overall, the findings reported here suggest that provision of sustained hFVIII-SQ production by hepatocytes may require due consideration, not only of the AAV5 vector dose used but also the strength of the

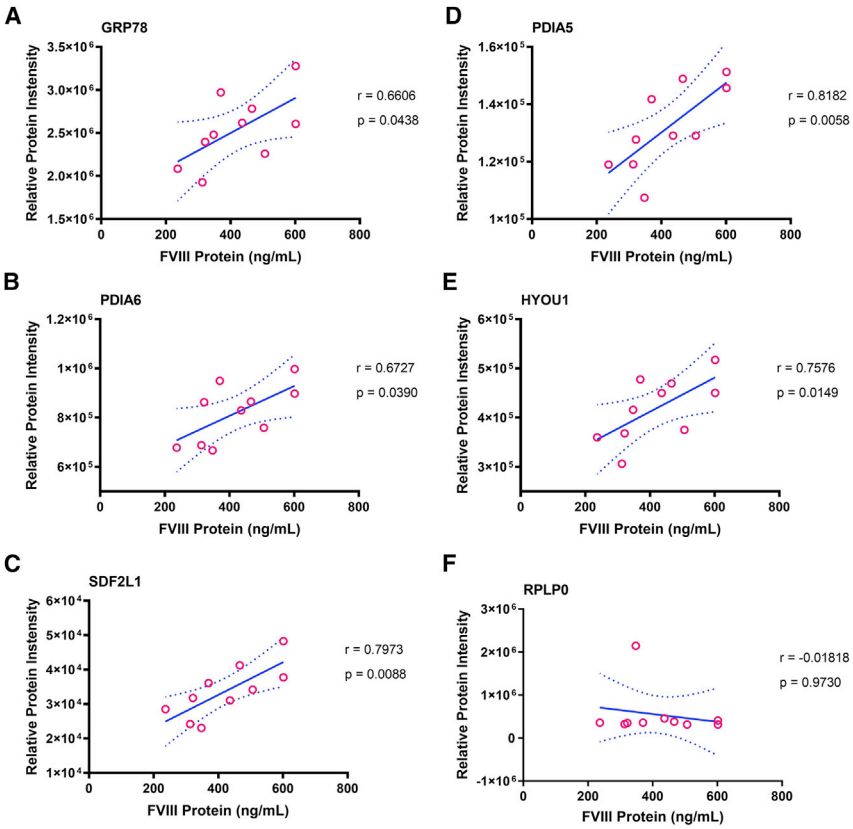

Figure 5. Relationship between Hepatic Expression of Molecular Chaperones and Circulating Plasma FVIII for 100ATGB

(A–F) Associations between circulating plasma hFVIII-SQ protein levels and the hepatic expression of (A) GRP78, (B) PDIA6, (C) SDF2L1, (D) PDIA5, (E) HYOU1, and (F) RPLP0, with 100ATGB measured by HRM proteomic analysis. Results are mean with confidence intervals n = 10 per group. GRP78, 78 kDa glucose-regulated protein; FVIII, factor VIII; HRM, hyper-reaction monitoring; HYOU1, hypoxia upregulated 1; PDIA5, protein disulfide isomerase family A member 5; PDIA6, protein disulfide isomerase family A member 6; RPLP0, ribosomal phosphoprotein P0; SDF2L1, stromal cell-derived factor 2-like protein 1.

associated promoter. A relatively strong promoter, such as 100ATGB, induces expression of hFVIII-SQ at relatively lower vector doses and consequently, fewer transduced hepatocytes to produce relevant levels of FVIII. However, the therapeutic window may be narrower, and it may induce adaptive UPR, which, if prolonged, may lead to apoptosis, loss of hepatocytes, and potentially, liver dysfunction and/or loss of transgene expression. Conversely, use of a weaker promoter, such as HLP, together with a relatively higher vector dose may distribute the expression burden to a greater number of transduced hepatocytes, thereby reducing the likelihood of an UPR. The findings may not apply to gene therapy-mediated production of intracellular proteins or proteins with simple folding and secretion mechanisms. Importantly, there is no evidence of liver dysfunction or cellular stress in mice treated with valoctocogene roxaparvovec, a gene therapy that employs the HLP promoter, at vector doses associated with production of normal to supraphysiological hFVIII-SQ levels.

MATERIALS AND METHODS

Constructs and AAV Vectors

In this preclinical study, 2 AAV5 hFVIII-SQ vector constructs were compared. Each vector construct contained a liver-specific promoter of differing strength (i.e., HLP [AAV5-HLP-hFVIII-SQ, BMN270, valoctocogene roxaparvovec] and 100ATGB [AAV5-100ATGB-hFVIII-SQ]). As described previously,[10] the expression cassette sequence also included a codon-optimized human BDD coagulation FVIII cDNA packaged into AAV5 viral particles using Sf9 host cells infected with helper and vector baculovirus[38] and a synthetic polyadenylation signal, overall flanked by AAV2 inverted terminal repeats (Figure 1). More specifically, the 100ATGB construct was composed of the following: an intact, 305-bp apolipoprotein E hepatic control region; the human alpha-1-antitrypsin (hAAT) promoter fragment used in the HLP promoter, described by Colosi et al.;[39] a chimeric intron that employs the splice donor from the first intron of hAAT and the last 131 bp of the human B-globin second intron; a hFVIII-SQ open reading frame; and the bovine growth hormone full 3′ untranslated region and polyadenylation site. The HLP construct is composed of the HLP promoter, as described by Colosi et al.,[39] the same hFVIII sequence, and a synthetic polyadenylation site based on rabbit B-globin, as described by Proudfoot and colleagues.[40]

Animals

All mouse experimentation was performed in accordance with institutional guidelines under protocols approved by the Institutional Animal Care and Use Committee of the Buck Institute (Novato, CA, USA). In these studies, 8-week-old male *RAG2*$^{-/-}$ mice were used (B6.129S6-Rag2tm1Fwa; Taconic, Hudson, NY, USA). AAV5-hFVIII-SQ vectors were prepared in vehicle (0.001% pluronic F-68 in Dulbecco's phosphate-buffered saline), and mice (n = 10 per group) received a single injection via the tail vein of vehicle alone, HLP, or 100ATGB at doses of 6×10^{12}, 2×10^{13}, or 6×10^{13} vg/kg.[10]

5 weeks following administration of the single vector dose, animals were deeply anesthetized with inhaled isoflurane and exsanguinated via cardiac puncture.[10] Blood was collected with sodium citrate anticoagulant (0.38% final concentration). Following cervical dislocation, liver samples were harvested. Median lobes were cut into 2 pieces and formalin fixed (10% formaldehyde), paraffin embedded (FFPE) and sectioned at 5 μm thickness for IHC analysis. The rest of the liver was divided into 3 tubes and snap frozen for biochemical analysis.

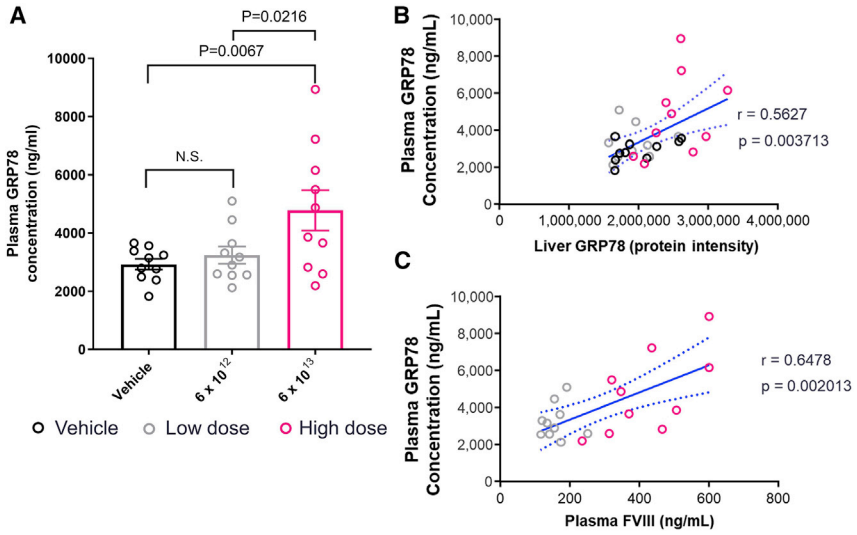

Figure 6. 100ATGB and Plasma and Liver Levels of GRP78

(A) Associations between plasma GRP78 concentration by dose of 100ATGB. (B and C) Relationship between plasma GRP78 and (B) liver GRP78 levels and (C) plasma FVIII levels. Liver GRP78 protein intensity measured by hyper-reaction monitoring mass spectrometry. Results are mean ± SEM or mean with confidence intervals n = 10 per group. FVIII, factor VIII; GRP78, 78 kDa glucose-regulated protein.

Study Measures

Plasma and liver levels of hFVIII-SQ protein were determined by sandwich ELISA for human-specific FVIII (Green Mountain Antibodies, Burlington, VT, USA), and liver FVIII-SQ DNA and RNA were determined by qPCR and reverse transcription followed by qPCR, respectively.[10] Immunofluorescence staining was performed to detect and localize hFVIII-SQ and GRP78 in liver sections, using 4′,6-diamidino-2-phenylindole (DAPI) as counterstain. Plasma levels of ALT were measured by fluorometric assay (Sigma-Aldrich, St. Louis, MO, USA), with detection using a FlexStation 3 multimode microplate reader (Molecular Devices, Sunnyvale, CA, USA).

ISH was used to detect hFVIII DNA in liver. FFPE mouse liver sections (5 μm) were collected on Superfrost Plus slides and a RNAscope ISH protocol performed using a Ventana Discovery Ultra Autostainer (Ventana Medical Systems, Tucson, AZ, USA), an RNAscope (Advanced Cell Diagnostics, Newark, CA, USA), a Universal 2.5 Reagent Kit Brown (catalog number 322200), and custom-generated FVIII DNA probes. Slides were dehydrated and mounted using Permount mounting medium and sections imaged on a Leica DM5000 microscope (Leica Microsystems, Buffalo Grove, IL, USA) using transmitted light-imaging settings, a 40× 0.75 HCX Plan Fluor objective, and a DFC550 camera. Four images were acquired per liver section: 2 capturing the portal vein area and 2 capturing the central vein area of the lobule. Total hepatocyte nuclei per image were counted and scored positive for hFVIII-SQ DNA if any signal (brown foci) was observed within the nucleus.

UPR

Selected recognized biomarkers of UPR were determined in the liver in animals administered the highest tested dose of each construct (6×10^{13} vg/kg): GRP78 and spliced XBP1s mRNA by RT-ddPCR, CHOP (loading control TATA-box binding protein), by western blot, and active caspase-3 by ELISA. Further groups of animals (n = 2 in each) received tunicamycin, thapsigargin, or staurosporine, all known inducers of ER stress, as "active" controls; tunicamycin and thapsigargin for XBP1s and GRP78 expression; and staurosporine for active caspase-3 expression. As GRP78 is endogenously expressed by all hepatocytes, immunofluorescent quantification of GRP78 was designed to detect any GRP78 signal above endogenous. With the use of liver sections from vehicle- and tunicamycin-treated mice (see below), the threshold for the GRP78 channel was set such that cells in the vehicle-treated control were negative, whereas those in tunicamycin-treated controls were positive.[10,41] Other positive controls for the induction of apoptosis were thapsigargin added to hepatocytes[10] and staurosporine, 1 μM added to HepG2 cells (Sigma-Aldrich; S6942), incubated for 3 h at 37°C, cells lysed, and lysate applied to active caspase-3 ELISA (R&D Systems, Minneapolis, MN, USA).

HRM Proteomic Analysis

With the use of a method adapted from Bruderer et al.,[42] a SWATH-MS (sequential window acquisition of all theoretical mass spectra)-like data-independent acquisition (DIA) method was used to establish various protein levels in mouse livers from animals treated with vehicle or 6×10^{12} or 6×10^{13} vg/kg of the 100ATGB vector. Chaperone proteins evaluated were PDIA4, PDIA5, PDIA6, MANF, DNAJC3, GRP78 (or HSPA5), HYOU1, SDF2L1, and RPLP0.

Liver samples were homogenized in Biognosys (Zurich, Switzerland) lysis buffer (20 μL or 40 μL per mg for naive liver or treated liver, respectively) using a TissueLyser II beadmill (QIAGEN, Redwood City, CA, USA) and stainless-steel grinding beads. Lysates were treated with benzonase and protein concentration measured with a bicinchoninic acid assay (Pierce; Thermo Fisher Scientific, Rockford, IL, USA), according to the manufacturer's instructions. Samples (50 μg of protein) were denatured using Biognosys Denature Buffer, reduced using Biognosys Reduction Solution for 1 h at 37°C, and alkylated using Biognosys Alkylation Solution for 30 min at room temperature while kept in the dark. Subsequently, digestion was carried out overnight at 37°C using trypsin (Promega, San Luis Obispo, CA, USA), with a protein:protease ratio of 50:1. Peptides were desalted using a C18 MicroSpin plate (The Nest Group, Southborough, MA, USA), according to the manufacturer's instructions, and dried down using a SpeedVac system. Peptides were resuspended in 20 μL of liquid chromatography (LC) solvent A (1% acetonitrile in

water + 0.1% formic acid [FA]), and "spiked" with Biognosys HRM kit calibration peptides. Peptide concentrations were then measured using an ultraviolet/visible (UV/VIS) spectrometer (SPECTROstar-Nano; BMG Labtech, Ortenberg, Germany).

To facilitate the generation of a spectral library from treatment-naive mouse liver, high pH reversed-phase fractionation was carried out prior to LC-tandem mass spectrometry shotgun measures. Here, treatment-naive liver peptides (60 µg) were diluted 4-fold in 0.2 M ammonium formate (pH 10) and applied to a C18 MicroSpin column (The Nest Group). The peptides were then eluted using buffer solutions containing 0.05 M ammonium formate and an increasing acetonitrile concentration (5%, 10%, 15%, 20%, 25%, and 50%), at pH 10. Eluates were dried down, resolved in 15 µL solvent A, and spiked with Biognosys HRM kit calibration peptides. Fractions 5% and 50% were pooled. For the shotgun measures, peptide samples (1.5 µg: liver fractions 10%, 15%, 20%, and 25%; 3.0 µg: liver fractions 5% and 50% pooled) were injected onto an in-house packed C18 column (Dr. Maisch Repro-Sil-Pur, 1.9 µm particle size, 120 Å pore size; 75 µm inner diameter, 50 cm length; New Objective, Woburn, MA, USA), installed into a Thermo Scientific Easy-nLC 1200 nano-LC system; this system was further connected to a Thermo Scientific Q Exactive HF mass spectrometer equipped with a standard nano-electrospray source. Solvent A was 1% acetonitrile in water + 0.1% FA, and solvent B was 15% acetonitrile in water + 0.1% FA. The nonlinear LC gradient was 1% to 55% solvent B in 120 min, followed by solvent B 55% to 90% for 10 s, 90% for 10 min, 90% to 1% for 10 s, and 1% for 5 min. To optimize resolution and acquisition speed, a modified TOP15 mass spectrometric method was used.[43] Mass spectrometric data were analyzed using MaxQuant 1.5.5.1 software (https://maxquant.org/), with the false discovery rate on peptide and protein level set to 1% and a murine UniProt fasta database (*Mus musculus*, 2015-08-28; https://www.ebi.ac.uk/pride/archive/projects/PXD007150).

For treated mouse liver samples, peptides (2 µg per sample) were injected onto an in-house packed C18 column, using the same solvent and detection systems as described above with 1 full-range survey scan; 22 DIA window HRM mass spectrometric data were analyzed using Spectronaut 10 software (Biognosys) and measures normalized using local regression normalization.[44] The assay library (protein library) generated was used for row-based data extraction with the false discovery rate on the peptide level set to 1%.

Data Analysis

Data for plasma and liver levels of protein, DNA, and RNA and expression of ER stress biomarkers were analyzed by two-tailed Student's t test and one-way analysis of variance (ANOVA) with a subsequent Fisher's least significant difference (LSD) post-test (typically n = 10 measures per group). Data are presented as mean (±standard deviation) and mean (±standard error of mean); a p value <0.05 is considered statistically significant.

Association between hepatic expression of molecular chaperone protein levels and circulating FVIII-SQ protein levels was calculated as Pearson correlation coefficient. Enrichment of annotation terms and pathways in top proteins was discovered using BaseSpace Correlation Engine (Illumina, San Diego, CA, USA).[45]

SUPPLEMENTAL INFORMATION

Supplemental Information can be found online at https://doi.org/10.1016/j.omtm.2020.07.005.

AUTHOR CONTRIBUTIONS

Conceptualization, S. Bunting and S.F.; Investigation, L.Z., L.X., R. Mahimkar, R. Murphy, B.Y., B.H., C.-R.S., N.G., H.A., C.E., D.H., S.L., W.C.M., C.V., J.V., and J.W.; Writing – Original Draft, S.F. and B.Y.; Data Analysis, Y.R. and J.V.; Writing – Review & Editing, S. Bunting, S. Bullens, and S.F.; Supervision, S. Bunting, S. Bullens, S.F., D.H., C.E., and G.K.Y. All authors contributed to manuscript development, revising it critically for important intellectual content and approving the final version for publication.

CONFLICTS OF INTEREST

C.E. and J.V. are employees of Biognosys AG, Schlieren, Switzerland, and have generated the data for this manuscript as work for hire. They declare no additional conflicts of interest. All other authors are employees of BioMarin Pharmaceutical, Novato, CA, USA.

ACKNOWLEDGMENTS

The authors thank Peter Colosi for designing the constructs. Medical writing support, including assisting authors with development of the outline and initial draft and incorporation of comments, was provided by Carl Felton, PhD, and Valerie Moss, PhD, ISMPP, CMPP, of Paragon, Knutsford, UK, and by Puneet Dang, PhD, of AlphaBioCom LLC, King of Prussia, PA, USA, and supported by BioMarin Pharmaceutical Inc, Novato, CA, USA in accordance with Good Publication Practice guidelines (https://www.acpjournals.org/doi/10.7326/M15-0288). The sponsor was involved in the study design, collection, analysis, and interpretation of data, as well as data checking of information provided in the manuscript. Ultimate responsibility for opinions, conclusions, and data interpretation lies with the authors. Development of this manuscript was supported by BioMarin Pharmaceutical Inc, Novato, CA, USA.

REFERENCES

1. Iorio, A., Stonebraker, J.S., Chambost, H., Makris, M., Coffin, D., Herr, C., et al. Data and Demographics Committee of the World Federation of Hemophilia (2019). Establishing the prevalence and prevalence at birth of hemophilia in males: a meta-analytic approach using national registries. Ann. Intern. Med. *171*, 540–546.

2. Peyvandi, F., Garagiola, I., and Young, G. (2016). The past and future of haemophilia: diagnosis, treatments, and its complications. Lancet *388*, 187–197.

3. Whelan, S.F., Hofbauer, C.J., Horling, F.M., Allacher, P., Wolfsegger, M.J., Oldenburg, J., Male, C., Windyga, J., Tiede, A., Schwarz, H.P., et al. (2013). Distinct characteristics of antibody responses against factor VIII in healthy individuals and in different cohorts of hemophilia A patients. Blood *121*, 1039–1048.

4. Jacobson, S.G., Cideciyan, A.V., Ratnakaram, R., Heon, E., Schwartz, S.B., Roman, A.J., Peden, M.C., Aleman, T.S., Boye, S.L., Sumaroka, A., et al. (2012). Gene therapy for leber congenital amaurosis caused by RPE65 mutations: safety and efficacy in 15 children and adults followed up to 3 years. Arch. Ophthalmol. *130*, 9–24.

5. van Til, N.P., de Boer, H., Mashamba, N., Wabik, A., Huston, M., Visser, T.P., Fontana, E., Poliani, P.L., Cassani, B., Zhang, F., et al. (2012). Correction of murine Rag2 severe combined immunodeficiency by lentiviral gene therapy using a codon-optimized RAG2 therapeutic transgene. Mol. Ther. *20*, 1968–1980.

6. Nathwani, A.C., Reiss, U.M., Tuddenham, E.G., Rosales, C., Chowdary, P., McIntosh, J., Della Peruta, M., Lheriteau, E., Patel, N., Raj, D., et al. (2014). Long-term safety and efficacy of factor IX gene therapy in hemophilia B. N. Engl. J. Med. *371*, 1994–2004.

7. Mendell, J.R., Sahenk, Z., Malik, V., Gomez, A.M., Flanigan, K.M., Lowes, L.P., Alfano, L.N., Berry, K., Meadows, E., Lewis, S., et al. (2015). A phase 1/2a follistatin gene therapy trial for becker muscular dystrophy. Mol. Ther. *23*, 192–201.

8. Duan, D. (2018). Systemic AAV micro-dystrophin gene therapy for Duchenne muscular dystrophy. Mol. Ther. *26*, 2337–2356.

9. Rangarajan, S., Walsh, L., Lester, W., Perry, D., Madan, B., Laffan, M., Yu, H., Vettermann, C., Pierce, G.F., Wong, W.Y., and Pasi, K.J. (2017). AAV5-Factor VIII gene transfer in severe hemophilia A. N. Engl. J. Med. *377*, 2519–2530.

10. Bunting, S., Zhang, L., Xie, L., Bullens, S., Mahimkar, R., Fong, S., Sandza, K., Harmon, D., Yates, B., Handyside, B., et al. (2018). Gene therapy with BMN 270 results in therapeutic levels of FVIII in mice and primates and normalization of bleeding in hemophilic mice. Mol. Ther. *26*, 496–509.

11. Malhotra, J.D., Miao, H., Zhang, K., Wolfson, A., Pennathur, S., Pipe, S.W., and Kaufman, R.J. (2008). Antioxidants reduce endoplasmic reticulum stress and improve protein secretion. Proc. Natl. Acad. Sci. USA *105*, 18525–18530.

12. Miao, H.Z., Sirachainan, N., Palmer, L., Kucab, P., Cunningham, M.A., Kaufman, R.J., and Pipe, S.W. (2004). Bioengineering of coagulation factor VIII for improved secretion. Blood *103*, 3412–3419.

13. Moussalli, M., Pipe, S.W., Hauri, H.P., Nichols, W.C., Ginsburg, D., and Kaufman, R.J. (1999). Mannose-dependent endoplasmic reticulum (ER)-Golgi intermediate compartment-53-mediated ER to Golgi trafficking of coagulation factors V and VIII. J. Biol. Chem. *274*, 32539–32542.

14. McIntosh, J., Lenting, P.J., Rosales, C., Lee, D., Rabbanian, S., Raj, D., Patel, N., Tuddenham, E.G., Christophe, O.D., McVey, J.H., et al. (2013). Therapeutic levels of FVIII following a single peripheral vein administration of rAAV vector encoding a novel human factor VIII variant. Blood *121*, 3335–3344.

15. Zolotukhin, I., Markusic, D.M., Palaschak, B., Hoffman, B.E., Srikanthan, M.A., and Herzog, R.W. (2016). Potential for cellular stress response to hepatic factor VIII expression from AAV vector. Mol. Ther. Methods Clin. Dev. *3*, 16063.

16. Lange, A.M., Altynova, E.S., Nguyen, G.N., and Sabatino, D.E. (2016). Overexpression of factor VIII after AAV delivery is transiently associated with cellular stress in hemophilia A mice. Mol. Ther. Methods Clin. Dev. *3*, 16064.

17. Merlin, S., Famà, R., Borroni, E., Zanolini, D., Bruscaggin, V., Zucchelli, S., and Follenzi, A. (2019). FVIII expression by its native promoter sustains long-term correction avoiding immune response in hemophilic mice. Blood Adv. *3*, 825–838.

18. Shahani, T., Covens, K., Lavend'homme, R., Jazouli, N., Sokal, E., Peerlinck, K., and Jacquemin, M. (2014). Human liver sinusoidal endothelial cells but not hepatocytes contain factor VIII. J. Thromb. Haemost. *12*, 36–42.

19. Zhang, W., and Xu, J. (2018). Adaptive unfolded protein response promotes cell survival in rifampicin-treated L02 cells. Int. J. Mol. Med. *41*, 2233–2242.

20. Oslowski, C.M., and Urano, F. (2011). Measuring ER stress and the unfolded protein response using mammalian tissue culture system. Methods Enzymol. *490*, 71–92.

21. Ji, C., Kaplowitz, N., Lau, M.Y., Kao, E., Petrovic, L.M., and Lee, A.S. (2011). Liver-specific loss of glucose-regulated protein 78 perturbs the unfolded protein response and exacerbates a spectrum of liver diseases in mice. Hepatology *54*, 229–239.

22. Dorner, A.J., Wasley, L.C., and Kaufman, R.J. (1990). Protein dissociation from GRP78 and secretion are blocked by depletion of cellular ATP levels. Proc. Natl. Acad. Sci. USA *87*, 7429–7432.

23. Li, R., Yanjiao, G., Wubin, H., Yue, W., Jianhua, H., Huachuan, Z., Rongjian, S., and Zhidong, L. (2017). Secreted GRP78 activates EGFR-SRC-STAT3 signaling and confers the resistance to sorafeinib in HCC cells. Oncotarget *8*, 19354–19364.

24. Lang, E., Pozdeev, V.I., Shinde, P.V., Xu, H.C., Sundaram, B., Zhuang, Y., Poschmann, G., Huang, J., Stühler, K., Pandyra, A.A., et al. (2018). Cholestasis induced liver pathology results in dysfunctional immune responses after arenavirus infection. Sci. Rep. *8*, 12179.

25. Corrigall, V.M., Bodman-Smith, M.D., Brunst, M., Cornell, H., and Panayi, G.S. (2004). Inhibition of antigen-presenting cell function and stimulation of human peripheral blood mononuclear cells to express an antiinflammatory cytokine profile by the stress protein BiP: relevance to the treatment of inflammatory arthritis. Arthritis Rheum. *50*, 1164–1171.

26. Girona, J., Rodríguez-Borjabad, C., Ibarretxe, D., Vallvé, J.-C., Ferré, R., Heras, M., et al. (2019). The circulating GRP78/BiP is a marker of metabolic diseases and atherosclerosis: bringing endoplasmic reticulum stress into the clinical scenario. J. Clin. Med. *8*, 1793.

27. Huang, F., Li, X., Zhao, N., Duan, L., and Chen, Y. (2018). Circulating GRP78 acts as a biomarker in the early diagnosis of lung cancer. Int. J. Clin. Exp. Pathol. *11*, 5223–5231.

28. Ma, X., Guo, W., Yang, S., Zhu, X., Xiang, J., and Li, H. (2015). Serum GRP78 as a tumor marker and its prognostic significance in non-small cell lung cancers: a retrospective study. Dis. Markers *2015*, 814670.

29. Panayi, G.S., and Corrigall, V.M. (2014). Immunoglobulin heavy-chain-binding protein (BiP): a stress protein that has the potential to be a novel therapy for rheumatoid arthritis. Biochem. Soc. Trans. *42*, 1752–1755.

30. Oikawa, D., Kitamura, A., Kinjo, M., and Iwawaki, T. (2012). Direct association of unfolded proteins with mammalian ER stress sensor, IRE1β. PLoS ONE *7*, e51290.

31. Bertolotti, A., Zhang, Y., Hendershot, L.M., Harding, H.P., and Ron, D. (2000). Dynamic interaction of BiP and ER stress transducers in the unfolded-protein response. Nat. Cell Biol. *2*, 326–332.

32. Fink, E.E., Moparthy, S., Bagati, A., Bianchi-Smiraglia, A., Lipchick, B.C., Wolff, D.W., et al. (2018). XBP1-KLF9 axis acts as a molecular rheostat to control the transition from adaptive to cytotoxic unfolded protein response. Cell Rep. *25*, 212–223.e4.

33. Poothong, J., Pottekat, A., Siirin, M., Campos, A.R., Paton, A.W., Paton, J.C., Lagunas-Acosta, J., Chen, Z., Swift, M., Volkmann, N., et al. (2020). Factor VIII exhibits chaperone-dependent and glucose-regulated reversible amyloid formation in the endoplasmic reticulum. Blood *135*, 1899–1911.

34. Pasi, K.J., Rangarajan, S., Mitchell, N., Lester, W., Symington, E., Madan, B., et al. (2020). Multiyear follow-up of AAV5-hFVIII-SQ gene therapy for hemophilia A. N. Engl. J. Med. *382*, 29–40.

35. Wei, W., Zheng, C., Zhu, M., Zhu, X., Yang, R., Misra, S., and Zhang, B. (2017). Missense mutations near the N-glycosylation site of the A2 domain lead to various intracellular trafficking defects in coagulation factor VIII. Sci. Rep. *7*, 45033.

36. Wei, W., Zhu, X., Yang, R., and Zhang, B. (2016). Characterization of missense mutations in factor VIII that lead to abnormal N-linked glycosylation. Blood *128*, 3764.

37. Manno, C.S., Pierce, G.F., Arruda, V.R., Glader, B., Ragni, M., Rasko, J.J., Ozelo, M.C., Hoots, K., Blatt, P., Konkle, B., et al. (2006). Successful transduction of liver in hemophilia by AAV-Factor IX and limitations imposed by the host immune response. Nat. Med. *12*, 342–347.

38. Clément, N., and Grieger, J.C. (2016). Manufacturing of recombinant adeno-associated viral vectors for clinical trials. Mol. Ther. Methods Clin. Dev. *3*, 16002.

39. Colosi, P.C., Nathwani, A., Mcintosh, J., and Tuddenham, E. (2016). Adeno-associated virus factor VIII vectors. US patent US9504762B2, filed September 12, 2013, and granted November 29, 2016 (United States Patent).

40. Levitt, N., Briggs, D., Gil, A., and Proudfoot, N.J. (1989). Definition of an efficient synthetic poly(A) site. Genes Dev. *3*, 1019–1025.

41. Wang, H., Wang, X., Ke, Z.J., Comer, A.L., Xu, M., Frank, J.A., Zhang, Z., Shi, X., and Luo, J. (2015). Tunicamycin-induced unfolded protein response in the developing mouse brain. Toxicol. Appl. Pharmacol. *283*, 157–167.

42. Bruderer, R., Bernhardt, O.M., Gandhi, T., Miladinović, S.M., Cheng, L.Y., Messner, S., Ehrenberger, T., Zanotelli, V., Butscheid, Y., Escher, C., et al. (2015). Extending the limits of quantitative proteome profiling with data-independent acquisition and application to acetaminophen-treated three-dimensional liver microtissues. Mol. Cell. Proteomics *14*, 1400–1410.

43. Scheltema, R.A., Hauschild, J.P., Lange, O., Hornburg, D., Denisov, E., Damoc, E., Kuehn, A., Makarov, A., and Mann, M. (2014). The Q Exactive HF, a Benchtop mass spectrometer with a pre-filter, high-performance quadrupole and an ultra-high-field Orbitrap analyzer. Mol. Cell. Proteomics *13*, 3698–3708.

44. Callister, S.J., Barry, R.C., Adkins, J.N., Johnson, E.T., Qian, W.J., Webb-Robertson, B.J., Smith, R.D., and Lipton, M.S. (2006). Normalization approaches for removing systematic biases associated with mass spectrometry and label-free proteomics. J. Proteome Res. *5*, 277–286.

45. Kupershmidt, I., Su, Q.J., Grewal, A., Sundaresh, S., Halperin, I., Flynn, J., et al. (2010). Ontology-based meta-analysis of global collections of high-throughput public data. PLoS ONE *5*, e13066.